Chapter 6

Results and Discussion

6.1 Introduction

This chapter focuses on high frequency range mould vibration on the die-cast A308 alloy to increase nucleation sites during melt solidification by fragmenting dendrites and Si particles with the turbulence created by the mechanical vibration. The performance of the as-cast and vibrated cast samples was addressed in terms of physical, metallurgical and mechanical features. Hence keeping that in mind, the chapter has been divided into four sections (a) Physical properties, (b) Metallurgical properties, (c) Mechanical properties and (d) Fractography. The chapter concludes with a summary of the microstructure, physical, and mechanical results.

6.2 Effects of high-frequency range horizontal mould vibration on the physical, metallurgical, and mechanical properties of die-cast A308 alloy

The present investigation analysed the effect of mould vibration using an indigenous vibrating setup on the physical, metallurgical, and mechanical properties of die-cast A308 alloy. The alloy was vibrated at a constant amplitude of 31μm at 75, 100, 125, and 150 Hz. The work aims to generate more nucleation sites during melt solidification by fragmenting dendrites and Si particles. To examine the changes in metallurgical characteristics (α-Al, secondary dendritic arm spacing (SDAS), length, width, and aspect ratio of eutectic Si particles) were studied using optical microscopy, scanning electron microscopy (SEM), and x-ray diffraction (XRD) analysis. It was observed that the size of α-Al, SDAS, length, width, and aspect ratio of eutectic Si particles were decreased by 47%, 53%, 65%, 12%, and 61%, respectively. The shape factor and density of the alloy were enhanced by 25% and 1.62% compared to stationary cast samples because of mechanical vibration treatment at an optimum frequency of 100 Hz. Mechanical testing findings demonstrated a 13%, 20%, 15%, and 20% increase in the parameters such as

yield strength (YS), ultimate tensile strength (UTS), % elongation (EL), and microhardness (HV) at 100 Hz when compared to the stationary cast sample. Grain refinement, uniformity of structure, improvement in the morphology of metallurgical characteristics, decreased porosities, and subsequent increase in density all contributed to the improvement. Tensile test samples with SEM fractography demonstrated transgranular brittle fracture and a few ductile rips.

6.3 Physical properties

6.3.1 Density, porosity and cooling rate

According to the mixing rule, the alloy's theoretical density was 2.503 g/cm^3, but an empirically observed density value was 2.481 g/cm^3. The porosity defect is the fundamental difference between the two. Mechanical properties can be severely hampered by porosity defects. Porosity is caused by gas precipitation from the melt during solidification or the inability to compensate for volumetric shrinkage due to insufficient feeding over the interdendritic zone. The experimental densities of the cast sample at stationary and vibratory conditions are shown in Table 6.1. The as-cast density value was the most minor compared to all the densities measured at as-cast (0 Hz) and higher frequencies (75-150) Hz. The continuous improvement in the vibrated casting density was mainly due to the reduction in porosity defect due to sufficient feed against volumetric shrinkage over solidification and the effective removal of dissolved hydrogen in the melt through degassing agent C_2Cl_6. Fig. 6.1(a-c) shows a gradual reduction in the porosity size. As demonstrated in Table 6.2, cooling is 13% quicker due to vibration. Porosity is also reduced by 56% due to improved mass feeding and reduced porosities. Consequently, an increase of 1.61% in the density was obtained at 100 Hz frequency.

Beyond 100 Hz, a slight decrease in the density was observed, possibly due to gas entrapment during extra turbulence caused by higher frequencies[46].

Table 6.1: The density of A308 alloy under (0-150) Hz frequencies

Applied frequency (Hz)	Experimental density measurements				Theoretical density of A308 Alloy (g/cm^3)
	Weight in air (g)	Weight in water(g)	Average density(g/cm^3)	Standard deviation	
0	13.554	8.595	2.482	0.002	
75	13.204	8.429	2.504	0.006	
100	14.238	9.106	2.523	0.010	2.503
125	13.756	8.748	2.513	0.012	
150	13.001	8.310	2.493	0.007	

Table 6.2: The cooling rate of A308 alloy under (0-150) Hz frequencies

Frequency / Hz	Temperature / °C		Solidification Time / Sec.	Cooling Rate / °C / Sec.
	Pouring Temp.	Freezing Temp.		
0	710	520	123	1.54
75	710	520	116	1.63
100	710	520	110	1.72
125	710	520	112	1.69
150	710	520	114	1.66

6.4 Metallurgical observations

Figure 6.1(a-e) shows the optical images of A308 alloy cast under stationary and vibratory conditions. The microstructural features, i.e., α-Al grains, eutectic silicon size, shrinkage porosity, and SDAS, were reduced due to the faster cooling rate and intense convection caused by the mechanical vibration as shown in Table 6.2 [92]. Figure 6.1(a) shows the optical image of the stationary cast (0 Hz) sample, the size of α-Al grains, eutectic silicon, and DAS are coarser with large interdendritic shrinkage porosity.

However, at 100 Hz frequency, Fig. 6.1(b-e) exhibits dramatically decreased α-Al grains, eutectic silicon, SDAS, and shrinkage porosity with homogeneous grain structure.

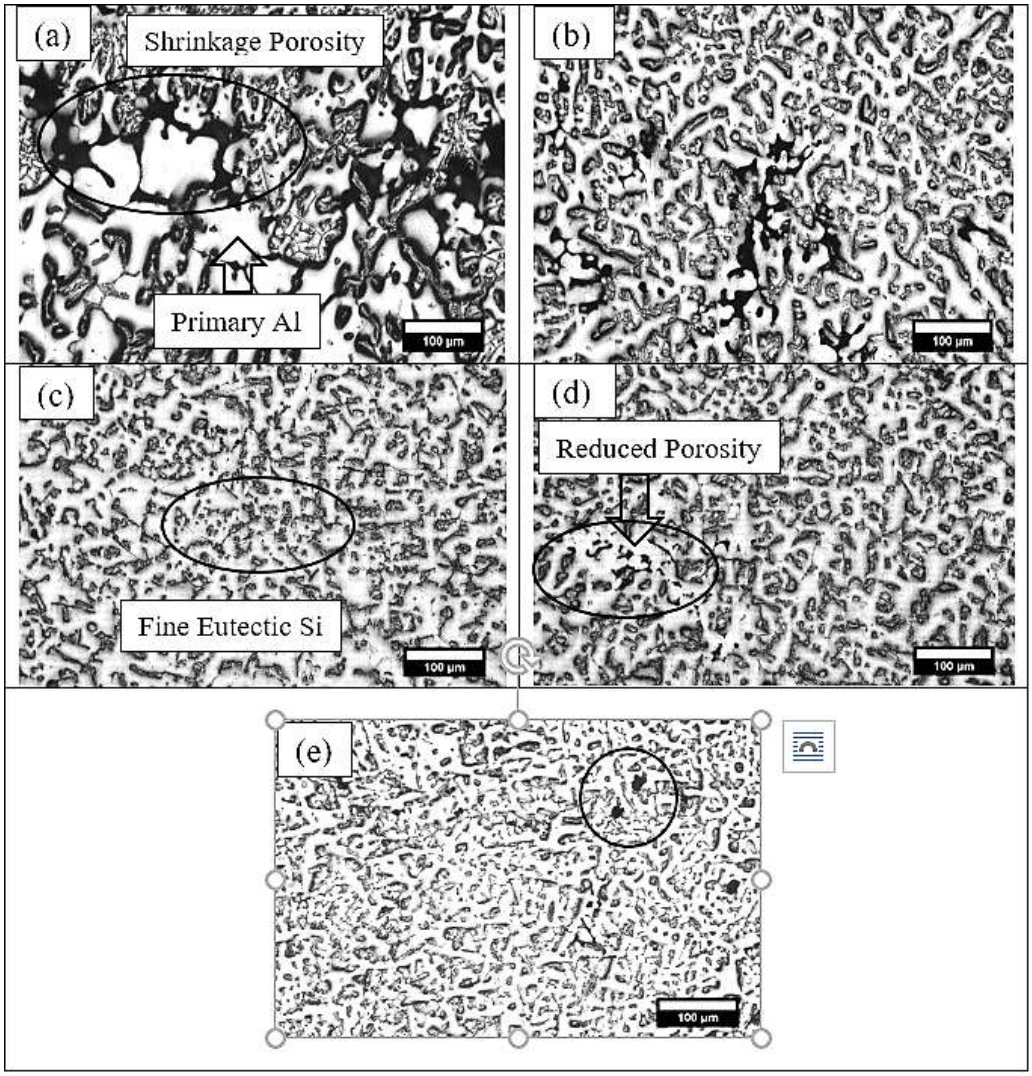

Figure 6.1: Microstructure of A308 alloys cast under (a) 0 Hz (Stationary condition); (b) 75 Hz; (c) 100 Hz; (d) 125 Hz; and (e) 150 Hz frequencies

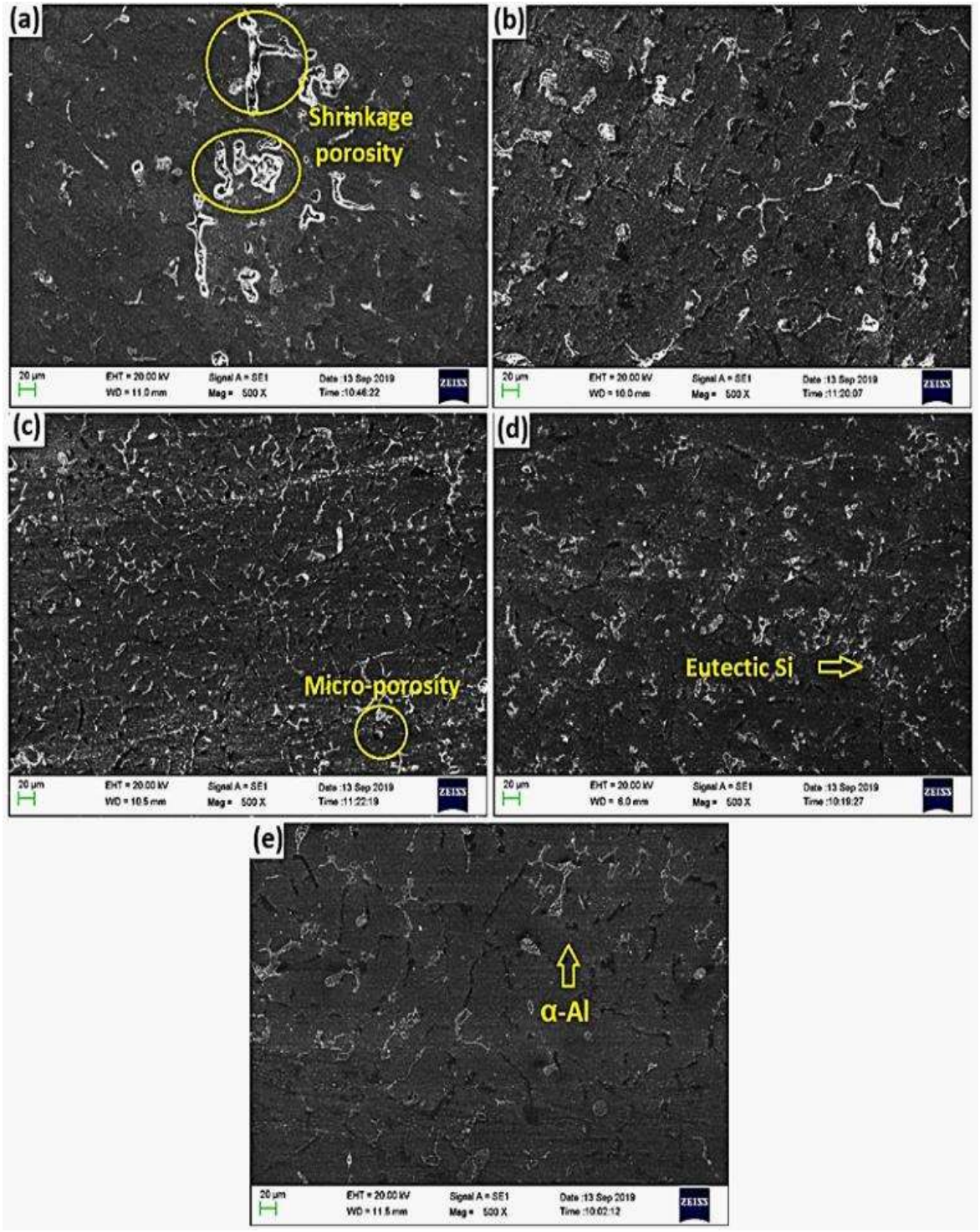

Figure 6.2: SEM micrographs of A308 alloys prepared under (a) 0 Hz (stationary condition); (b) 75 Hz; (c) 100 Hz; (d) 125 Hz; and (e) 150 Hz frequencies

However, when the frequency rose further, the size of the α-Al and SDAS grains grew somewhat, and the basic morphology of the α-Al grains deteriorated. Dendritic

fragmentation may also be seen in SEM micrographs of castings made in the (75-150 Hz) frequency range. As seen in Figures. 6.1(a-e) and 6.2(a-e), typical coarse columnar dendrites vanished and were distributed evenly along with refined Al-Si eutectic phases. Mechanical vibration produced an equiaxed, refined, and equally distributed non-dendritic microstructure. Finally, at 100 Hz frequency, it was concluded that the flake-shaped silicon transformed into fibrous-shaped silicon due to forced convection and rapid solidification as mould vibration-induced forced convection caused further dendrite fragmentation [92]. Simultaneously, an external force acted on the columnar dendrite arms in the direction of melt flow, and adequate fragmentations allowed more nucleation and grain multiplication producing a higher degree of refinement [4].

6.4.1 Morphology of the metallurgical features

The quantitative morphological changes of average α-Al grain size, SDAS, shape factor, length, width, and aspect ratio of Si particles under varying frequencies (0-150 Hz) were summarised in Table 6.3. Mould vibration decreased α-Al, SDAS, length, width, and aspect ratio of Si particles values, whereas the shape factor increased as the vibration frequency increased. At 100 Hz, the α-Al, SDAS, length, width, and aspect ratio of Si particles showed the lowest values, and they are 47%, 53%, 65%, 12%, and 61% lower than sample cast without vibration, respectively. Moreover, the shape factor showed the highest value at 100 Hz, and a 25% improvement was observed compared to samples cast without vibration. The increase in vibration frequency beyond 100 Hz slightly increases the average values of α-Al grain size, SDAS, length, width, and aspect ratio of Si particles [3].

On the other hand, the shape factor reduces, owing to the strong turbulence in the melt, as indicated in Table 6.3 [3]. The mould vibration causes a higher cooling rate, about 13% faster than the as-cast state. The forced convection effect of mould shaking increases

the heat transmission coefficient is increased by the forced convection effect caused by mould shaking [46]. Furthermore, as the frequency of vibration increases, so does the intensity of vibration. Consequently, the amount of shear force generated is more significant than at lower frequencies[84]. High shear force improves the flowability, shape factor, and dendritic fragmentation, widens the width and shortens the length of the eutectic silicon, and the porosity of the casting is reduced. The aspect ratio for equiaxed grain size is close to 1. For columnar grains, it is greater than 1. The shape factor value of 1 represents the complete globularity of the α-Al phase. The shape factor represents the globularity of grains; if the shape factor's value is close to 1, it means the grain is spherical[3, 85].

Table 6.3: Effect of mechanical vibration (0-150) Hz under on the morphology of the metallurgical feature

Frequency /Hz	Avg α-Al size/ µm	Avg SDAS/ µm	Avg. Shape factor (SF) = $4\pi A/P^2$	Avg. length of eutectic Si / µm	Avg. width of eutectic Si / µm	Avg. Aspect ratio of eutectic Si = L_{max}/L_{min}
0	106.91±21.15	76.67±12.7	0.61±0.01	45.86±8.44	7.31±1.52	6.27±1.05
75	63.22±10.45	48.5±7.52	0.72±0.01	16.99±4.07	6.66±1.31	2.54±0.34
100	56.62±9.61	35.9±6.23	0.81±0.02	16.19±2.85	6.53±1.68	2.47±0.33
125	58.32±9.23	38.89±6.62	0.75±0.01	16.72±3.11	6.73±2.01	2.48±0.49
150	59.79±9.89	39.35±6.81	0.76±0.02	17.06±3.61	6.85±1.21	2.49±0.54

Notes: Where L_{max}= Maximum length; L_{min}= Minimum length; A= Area; P= Perimeter

6.4.2 X-ray diffraction (XRD) analysis

PCPDFWIN-2013 software was used to analyse X-ray diffraction to determine the primary and secondary phases present in the alloy. The presence of Al, Si, Al_2Cu, and $Fe_{1.7}SiAl_4$ was confirmed by XRD analysis, as shown in Figure 6.3. The elements in the examined cast samples are Al, Si, Cu, and Fe, along with the possible formation of intermetallic compounds such as Al_2Cu and $Fe_{1.7}SiAl_4$. During solidification, copper reacts with aluminium to produce the Al_2Cu intermetallic phase. Al_2Cu can precipitate in block form from the liquid as soon as its Cu concentration reaches 53.5 wt. %, particularly in the presence of the β-Fe phase, or in eutectic (Al_2Cu + Al), or a combination of both, depending on the cooling rate and local concentration of segregated Cu atoms. Typically, the copper phase forms as small pockets of blocky Al_2Cu nucleating on pre-existing β-Fe platelets.[31] Intermetallic compounds are usually brittle and have a high melting point. They provide a compromise between ceramic and metallic properties [87].

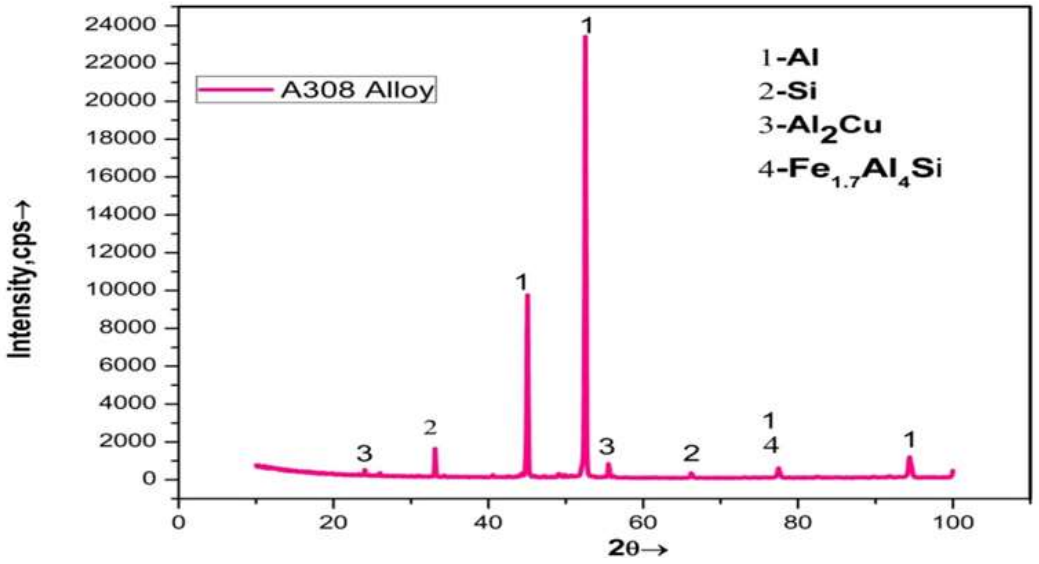

Figure 6.3: X-ray diffraction pattern of A308 alloy

6.4.3 Energy dispersive spectrometer (EDS) analysis

The component phases and compositions were confirmed using SEM and EDS methods, as shown in Figure 6.4. The goal of the elemental analysis was to determine the element weight percentage and EDS spectrum at two sites in Figure 6.4(a–b). Elements including Al, Si, Cu, and Fe are present in Figure 6.4(a), confirming the development of intermetallics such Fe-Si-Al and Al_2Cu. Similarly, Al, Si, Mn, and Cu, in addition to Fe, were verified in Figure 6.4(b), indicating the production of intermetallics such as $Fe_{1.7}SiAl_4$ and Al_2Cu. These findings matched with XRD analysis [88].

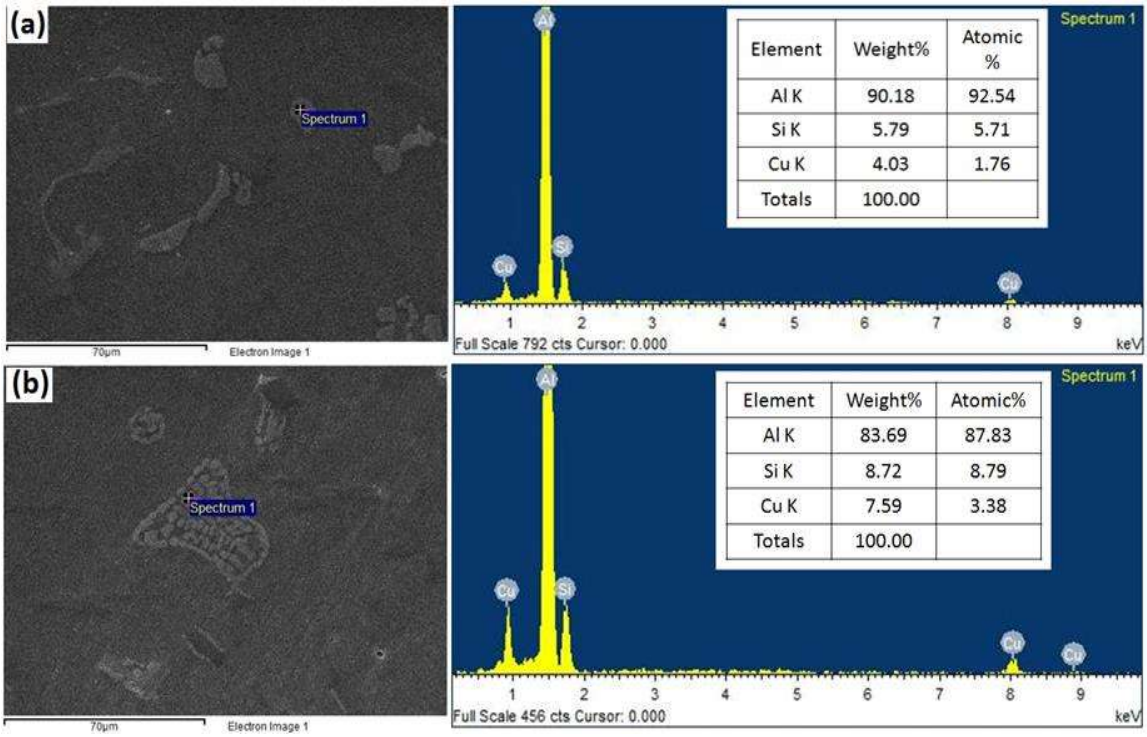

Figure 6.4: EDS analysis of A308 alloy cast under the as-cast condition

6.5 Mechanical properties

6.5.1 Tensile properties

Tensile tests were performed to assess the mechanical characteristics' improvement and investigate the casting's fracture behaviour under mechanical vibration. Table 6.4 shows the tensile characteristics of cast samples under stationary and vibratory castings. By

increasing the frequency level up to 100 Hz, the mechanical characteristics of the vibratory cast samples, such as yield strength (YS), ultimate tensile strength (UTS), percentage elongation (%EL), and microhardness (HV) of the alloy, improved. The results showed that the maximum percentage improvement in YS, UTS, % EL and HV was 13, 20, 15, and 20% compared to the stationary cast samples. These improvements were observed due to significant refinement of grain size. As per the Hall-Petch equation (6.1), the YS of the alloy is inversely proportional to the average grain size [89].

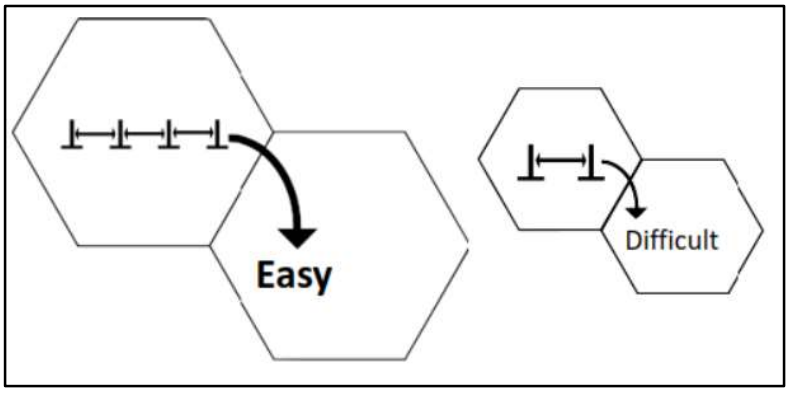

Figure 6.5: Pile-up of dislocations at grain boundary

As shown in figure 6.5, the schematic illustrates the idea of dislocation pile-up and how it impacts the material's strength. Because more dislocations can accumulate in a material with larger grains, there is a greater driving force for dislocations to travel from one grain to another. Because a larger grain requires less force to move a dislocation than a smaller grain does, materials with smaller grains show higher yield stress.

$$\sigma_y = \sigma_o + k_y\, d^{-1/2} \qquad (6.1)$$

where σy is yield stress, σo is a material constant for starting stress for dislocation movement, ky is the strengthening coefficient (a constant particular to each material), and d is the average grain diameter.

Other factors, such as a decrease in porosity percentage, the aspect ratio of eutectic Si particles, low SDAS, increase in shape factor and density, also attributed to the enhancement of mechanical properties of the cast alloy at 100 Hz frequency as compared with low frequency or as-cast (stationary) samples.

Table 6.4: Mechanical properties of cast samples under (0-150) Hz frequencies

Mechanical vibration parameters			YS/MPa	UTS/MPa	%El	HV
Power Input/V	Amplitude/µm	Frequency/Hz				
7.6	0	0	98.50±3.50	148.50±4.01	3.30±0.31	75±2.08
7.6	31	75	102.6±1.50	170.95±2.21	3.00±0.35	81±4.04
7.6	31	100	110.9±2.50	178.68±3.26	3.80±0.25	90±3.06
7.6	31	125	104.60±3.00	174.82±3.07	3.2 ±0.30	85±3.51
7.6	31	150	101.2±2.56	164.10±2.91	2.80±0.30	81±2.52

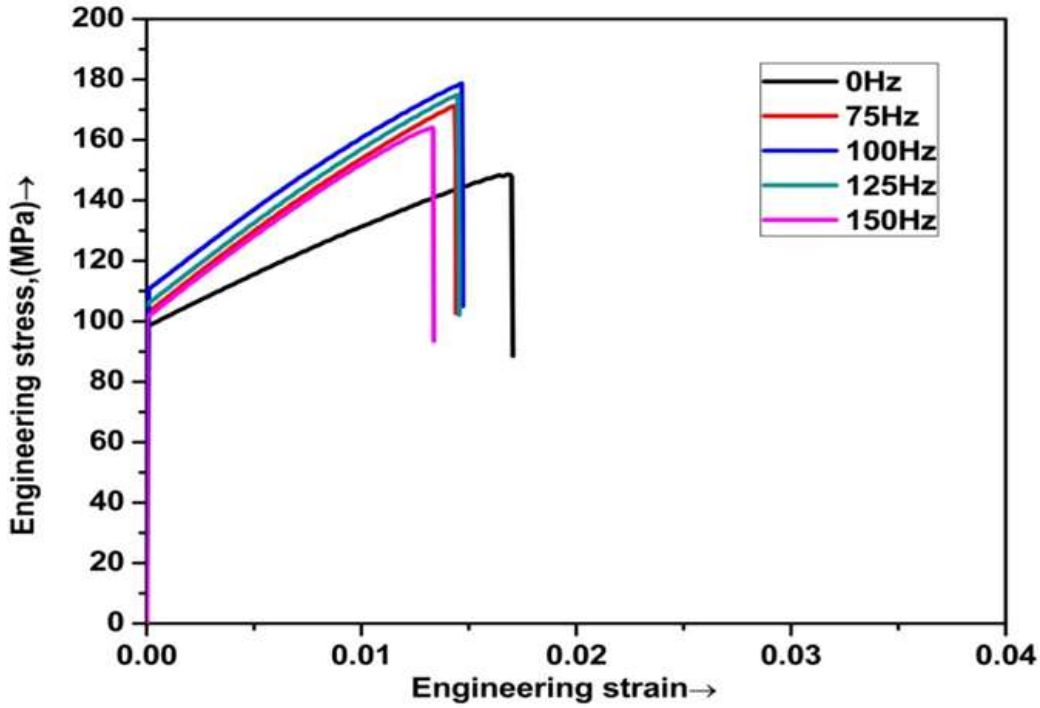

Figure 6.6: Engineering stress-strain diagram of A308 alloy's cast samples prepared under (a) 0 Hz (stationary condition); (b) 75 Hz; (c) 100 Hz; (d) 125 Hz; and (e) 150 Hz frequencies

A typical engineering stress-strain curve of A308 alloy cast under stationary and vibratory casting conditions is shown in Figure 6.6. In a static cast condition, the UTS value was 148 MPa (Figure 6.6). When the frequency was increased to 100 Hz, the UTS value increased to 178 MPa, a 20% improvement over the stationary casting. The combined impact of grain refinement, homogeneity, and non-dendritic structure, reduced porosity, enhanced density, and significant change in the morphology of metallurgical characteristics at 100 Hz contributed to the 20% increase in UTS value. Varun et al. found the intensity of vibration causes inner casting defects to decrease to help in increasing the mechanical properties [98].

6.5.2 Microhardness

The findings of microhardness tests conducted in both stationary and vibratory situations are provided in Table 6.4. The hardness value in stationary circumstances was 75 HV,

much lower than all hardness values found at various vibratory conditions, owing to the coarser grain size, eutectic silicon particles, and bigger dendrites cells. The highest hardness value, 90 HV, was observed at a frequency of 100 Hz, indicating a 20% increase in hardness value. Table 6.3 shows that substantial refinement in the grain size, i.e., 47%, increased the hardness rating. An increase in microhardness was observed due to a much-refined microstructure attributed to a faster cooling rate, i.e., 13% extra compared to stationary cast condition shown in Table 6.2 [98]. The application of mechanical vibration during melt solidification causes dendritic fragmentation. These fragmented arms acted as new nucleation sites and instigated further nucleation; consequently, the non-dendritic and equiaxed microstructure was obtained, which resulted in a uniformly distributed fine-grained structure [47]. Similarly, at 100 Hz, due to rapid solidification and forced convection, refined eutectic silicon, reduced α-Al phase phases, and intermetallic phases like Al_2Cu, $Fe_{1.7}SiAl_4$ got dispersed uniformly in the alloy. It caused substantial improvement in mechanical properties also [63].

6.6 Fractography

After the tensile test, the broken samples were obtained to evaluate the A308 alloy's fracture behaviour. Figures 6.7(a-e) illustrate SEM fractographs of broken surfaces. At stationary cast conditions Figure 6.7(a), SEM fractography of broken tensile test samples revealed coarse dendrites, substantial interdendritic shrinkage, and gas porosities. The broken sample pieces obtained at 75 Hz had a grape-like dendritic structure with microporosity and trans-granular fracture, as illustrated in Figure 6.7(b). The fracture surface shows microcracks, cleavage facets, and ductile tears at a frequency of 100 Hz. The appearance of ductile tears suggests that the alloy's ductility has improved. Hence, the alloy had a higher ductility than the other samples. It could be attributed to grain

refinement and lower SDAS, which contribute to the alloys' enhanced ductility, as shown in Figure 6.7(c).

At 150 Hz, the fracture images presented in Fig. 6.7(e) showed partial ductile tearing and Si particle pullout. Due to dendritic fragmentation and grain multiplication, most refined grain structures were observed at a higher frequency (100 Hz). Subsequently, mechanical properties were enhanced [3]. The fracture occurred along with hard eutectic silicon and Fe-intermetallic phases, showing the brittle facets, as shown in Figure 6.7(d-e). Some Si particles are pullout from the matrix during tensile test operations. With the increased vibration ranging from (125-150) Hz, the coarse dendrites and shrinkage porosities were significantly reduced, as illustrated in Figure 6.7(b-e). Most of the fractured surfaces show a brittle fracture, as shown in Figure 6.7(c-d). Cleavage and brittle facets can easily be seen throughout the fractured surfaces in the brittle fracture mode, as illustrated in Figure 6.7(b-e) [85, 92].

The fractured surface morphology also shows intermetallic phases' debonding (Eutectic Si particles, Al_2Cu, and other impurities like Mn, Fe, Ni) from the Al-matrix, causing initiation of crack propagation. Figure 6.7 (b-d) shows the intermediate casting mode of vibration at 75 and 125 Hz. The fractured surfaces show the brittle fracture mode with micro-cracks, micro-voids, brittle facets, and ductile tearing, indicating the mixed-mode fracture behaviour [92].

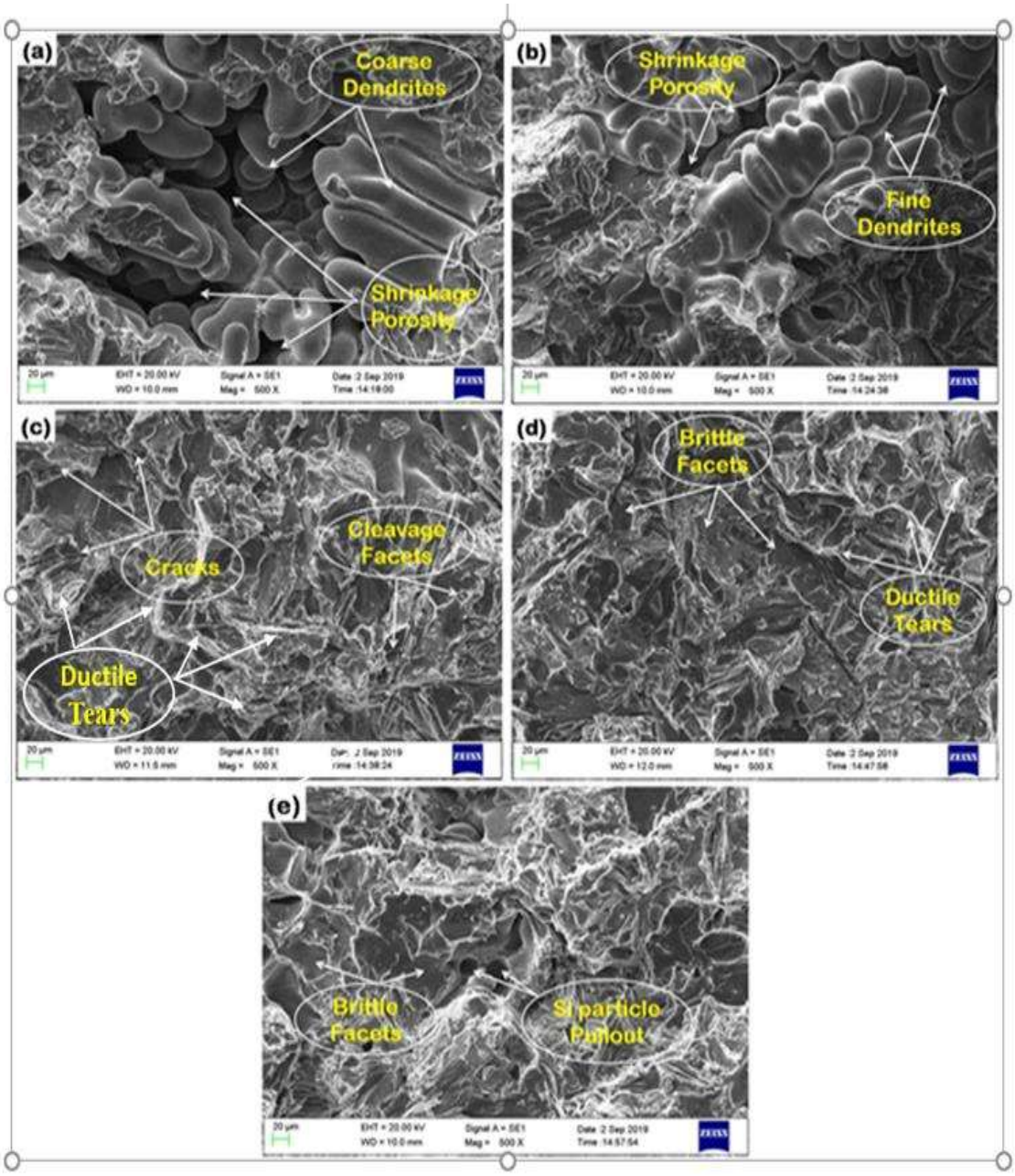

Figure 6.7: SEM Fractographs of A308 alloy tensile test samples cast under (a) 0 Hz (stationary condition); (b) 75 Hz; (c) 100 Hz; (d) 125 Hz; and (e) 150 Hz frequencies.

6.7 Summary

The effect of horizontal mechanical mould vibration effect on A308 alloy's physical, metallurgical, and mechanical properties was investigated, and the following conclusions were made:

1. XRD analysis shows elements like Al, Si, and Cu hard particles or impurities like Fe, Mn, Mg, and intermetallics, e.g., $Fe_{1.7}SiAl_4$ and Al_2Cu, which were also detected by EDS analysis.
2. At 100 Hz frequency, 13% improvement in cooling rate due to forced convection and 56% reduction in porosity due to better mass feeding and reduced porosities causes the density to increase by 1.61% as compared to conventional casting.
3. At 100 Hz frequency α-Al, SDAS, length, width, and aspect ratio of eutectic Si particles were reduced by 47%, 53%, 65%, 12%, and 61%, respectively. The shape factor increased by 25% compared to stationary cast samples due to rapid cooling and turbulence generated by mechanical vibration.
4. The fragmentation of dendritic structure to non-dendritic structure, as well as refinement of the morphology of the microstructure, leads to the improvement in the YS, UTS, %EL, and HV by 13, 20, 15, and 20%, respectively, as compared to the stationary cast sample at 100 Hz.
5. The SEM fractography of tensile test samples showed transgranular brittle fracture with cleavage and brittle facets throughout the stationary and vibratory casting surfaces. However, at higher frequencies (100-150 Hz), the fracture samples showed some ductile tears also.